Localization and Magnetic Field Effects in Heisenberg Chains with Generalized Exponentially Correlated Disorder

M. S. S. Junior[a], D. B. da Fonseca[b], F. Moraes[b], A. L. R. Barbosa[b], G. M. A. Almeida[a], F. A. B. F. de Moura[a]

[a] *Instituto de Física, Universidade Federal de Alagoas, 57072-970, Maceió-AL, Brazil*
[b] *Departamento de Física, Universidade Federal Rural de Pernambuco, Recife-PE, 52171-900, Brazil*

Abstract

We examine the properties of the one-magnon eigenstates in a Heisenberg chain with correlated disorder in the presence of a magnetic field that increases linearly along the chain. The disorder distribution is tailored to have intrinsic generalized exponential correlations. We further analyze the dynamic localization of an initial wave packet and discuss how it is influenced by the correlations and the strength of the magnetic field. We find that localized eigenstates are predominant when the correlated disorder is characterized by a slower dependence of the effective correlation length on the system size. In contrast, when the effective correlation length increases at least with the square root of the system size, low-energy eigenmodes undergo a transition to nearly delocalized modes. We go further to analyze the impact of a linearly varying magnetic field on the system dynamics. An initial Gaussian wave packet is shown to exhibit dynamic localization, characterized by an oscillatory behavior reminiscent of Bloch oscillations at specific correlation levels, before being damped in the long time limit. Our findings advances the understanding of localization and transport properties in the field of coherent magnonics as contributes to the design of correlated disordered media.

1. Introduction

A well-established result in condensed-matter physics is that free particles in 1D and 2D lattices with uncorrelated disorder experience Anderson localization across the entire energy spectrum. Additionally, it is understood that correlated disorder can evade these effects by altering the localization length of certain modes and enabling the coexistence of localized and extended modes, possibly with well-defined mobility edges [1]. In reality, correlations are always present

Email address: fidelis@fis.ufal.br (F. A. B. F. de Moura)

in a disorder distribution to some degree. This and the possibility of designing and manipulating disorder for specific purposes have driven research towards investigating the consequences of correlated disorder in the transport properties of a variety of systems [2, 3, 4, 5]. Experimental realizations of correlated disorder have been reported in waveguide arrays [6], cold atoms [7, 8], dielectric nanodisk arrays [9], and coupled lasers [10].

Localization properties of waves in low-dimensional systems with correlated disorder have been receiving significant attention [11, 12, 13, 14, 15, 16, 17, 18, 19, 20, 21, 22, 23, 24, 25, 26, 27, 1, 28]. For instance, the reduction of thermal conductivity in insulators and semiconductors by incorporating correlations within intrinsic disorder was studied in [11]. Simulations with isotropic long-range spatial correlations in defect distributions demonstrated significant reductions in phonon lifetimes and thermal conductivity, potentially by an order of magnitude at room temperature. This research proposed a framework to control thermal transport via structural correlations and identified optimal correlation forms to minimize thermal conductivity. In [13], it was shown that correlated disorder significantly affected photonic transport: quasiperiodic lattices maintained nearly ballistic transport, amorphous lattices exhibited partially destroyed transport, and completely random lattices deviated entirely from ballistic transport. The photon spreading coefficient varied with the characteristic length scale of the disorder, distinctly classifying disorder types in materials. In Ref. [14], a robust and unusual multifractal regime was reported in a one-dimensional quantum chain with exponentially correlated disorder above a certain threshold disorder strength. Prior to this regime, there are mixed and extended regimes at weaker disorder strengths. Such multifractal states differ from conventional ones in that they are uniformly spread over a continuous chain segment, with lengths scaling non-trivially with system size. This anomaly affects dynamics, leading to the ballistic transport of a localized wavepacket, unlike the typically subdiffusive transport observed in multifractal systems.

A novel paradigm of dynamical quantum phase transitions driven by changes in internal spatial disorder potential correlations was proposed in [18]. Anomalous phase transitions due to infinite disorder correlation and quench dynamics between random and pure system Hamiltonians were explored, including phase transitions for prequench white-noise potential and delocalization signatures in the correlated Anderson model. In Ref. [19], the superconductivity characteristics of a disordered superconductor were investigated using an attractive Hubbard lattice Hamiltonian with point interaction, designed to model s-wave Cooper pairing. The study examined the effect of spatial correlations of disorder on the density of states and the superconducting coupling constant matrix elements. Surface superconductivity persistence in the presence of weak to moderate bulk disorder was demonstrated in [22]. Notably, under moderate disorder conditions, the surface critical temperature can increase further, depending on disorder intensity and correlation. In [24], the coupling of a disordered chain (localized states) with a free chain (extended states) showed distinct localization behaviors in overlapped and non-overlapped regimes without a phase transition. Significant suppression of localization in the non-overlapped regime, influenced

by inter-chain coupling strength and energy shift between chains, suggested localization lengths comparable to system sizes even under strong disorder, verified through extensive numerical methods. In [26], localization-delocalization transitions in double chain models with long-range correlation were investigated. Exact positions of mobility edges were identified, consistent with transfer matrix numerical results. A second-order quantum phase transition due to interchain correlation in on-site energy was identified, indicated by a critical exponent jump in localization length. Without interchain correlation, the critical exponent was determined by the chain with lesser long-range correlation.

In the context of quantum information processing and magnonics [29], the transfer of a magnon state across a quantum Heisenberg model with correlated disorder and random magnetic fields was investigated in [27]. The disorder followed a power-law spectrum distribution, while magnetic fields were uniformly random. Numerical investigations focused on the interplay between disorder and correlation in transferring the magnon state across the chain. Transfer fidelity and end-to-end concurrence were evaluated to identify conditions under which high-fidelity state transfer protocols were feasible despite the presence of disorder.

In this work, we focus on the spectral and dynamical properties of one-magnon states in the Heisenberg model assuming that coupling between spins (exchange interaction) follows a disordered distribution containing exponential correlations. The disorder distribution features a generalized correlation length defined as a nonlinear function of the system size. Broadly speaking, most correlated disorder models in the literature can be divided into two categories: (i) models that exhibit a typical correlation length (with exponential decay or another form with a characteristic length), or (ii) models whose correlation function typically lacks a characteristic length (such as power-law or Bessel functions). These categories have been widely investigate by members of this work (see e.g. [27, 28, 30, 31, 32]). Here, we delve into a third class of correlated disorder, where the system has a characteristic length, but this length has a controllable dependence on the system size. This is one of the main distinguishing features of our model. We perform a systematic study of the transport properties of the system via exact diagonalization of the Hamiltonian and using the transfer matrix formalism. Additionally, we investigate the oscillatory dynamics of spin waves in the presence of a linear magnetic field. We show that, for certain levels of correlation, the packet became dynamically localized with an oscillatory behavior reminiscent of Bloch oscillations. Our findings deepen the knowledge of localization and transport properties of magnetic systems in correlated disordered media, which are promising platforms for, e.g., magnonics [29].

2. Model and formalism

We consider a disordered chain of N Heisenberg spins ($S = 1/2$). In our model, a magnetic field perpendicular to the chain direction is denoted by $\vec{H}_n$

at each spin. The Hamiltonian for this model is given by:

$$\mathcal{H} = -\sum_{n=1}^{N} \Big[J_n \vec{S}_n \cdot \vec{S}_{n+1} + \vec{H}_n \cdot \vec{S}_n \Big], \tag{1}$$

where $\vec{S}_n$ are the local spin operators acting on site n, J_n represents the exchange couplings connecting sites n and $n+1$. The magnetic field is defined long the $z-$direction as $\vec{H}_n = [(\nu_B \eta H_0) n]\vec{z} = (Hn)\vec{z}$ [30, 33]. Therefore, its intensity grows linearly with the distance n from left edge of the chain. We assume that J_n is given by a generalized exponentially correlated disorder distribution. To build such a sequence, we initially generate Z_n defined as:

$$Z_n = \sum_{k=1}^{N} \Big(e^{-|n-k|/L_0} \Big) R_k, \tag{2}$$

where R_k are random numbers uniformly distributed within the interval $[-0.5, 0.5]$. The generalized correlation length L_0 is given by $L_0 = bN^a$, where a and b are tunable parameters. It is important to note that the points $a = 0$ and $b = 0$ are not included in the definition presented in the previous equation. Further, we normaliz Z_n to keep $\langle Z_n \rangle = 0$ and $\langle Z_n^2 \rangle - \langle Z_n \rangle^2 = 1$. The spin coupling distribution is therefore generated as $J_n = 2 + \tanh(Z_n)$.

Let us address the series of J_n and its dependence on the values of a and b. We start by computing the autocorrelation function defined as $C(r) = [\langle J_n J_{n+r} \rangle - \langle J_n \rangle \langle J_{n+r} \rangle] / [\langle J_n^2 \rangle - \langle J_n \rangle^2]$. In Fig. 1, we display $C(r)$ as a function of r for several values of a and b. We observe that for $a \to 0$ and $b \to 0$, the function $C(r)$ seems to become negligible for $r > 0$, i.e., the disorder distribution becomes uncorrelated. For large a and b, the autocorrelation function exhibits an exponential decay at non-zero distances ($r > 0$).

The primary focus of our work is to understand the effect of those correlations on the eigenstate properties of the Heisenberg model described above. In particular, we are interested in studying the one-magnon subspace of this Hamiltonian. The ferromagnetic ground state composed of all spins pointing in the same direction is represented by $|0\rangle$. Then, $|n\rangle = S_n^+ |0\rangle$ describes a single spin flipped at site n. The eigenstates of the Hamiltonian are therefore given by $|\Psi^j\rangle = \sum_{n=1}^{N} f_n^j |n\rangle$, where the coefficients f_n^j satisfies the equation [30, 34]

$$(J_n + J_{n-1}) f_n^j - J_n f_{n+1}^j - J_{n-1} f_{n-1}^j + 2H_n f_n^j = 2E_j f_n^j. \tag{3}$$

By expressing the previous equation in matrix form and diagonalizing it we can determine the eigenfunctions $\{f_n^j\}$ and eigenvalues $\{E_j\}$. Then, the density of states reads $DOS(E) = \sum_j \delta(E - E_j)$. We will also be interested in the participation ratio, defined by $P_j = \Big[\sum_{n=1}^{N} |f_n^j|^4 \Big]^{-1}$. It is important to note that P_j remains constant for localized states and is proportional to N for extended states [1]. In general, calculations of the participation function requires many averages. Therefore, our study do not focus directly on the participation

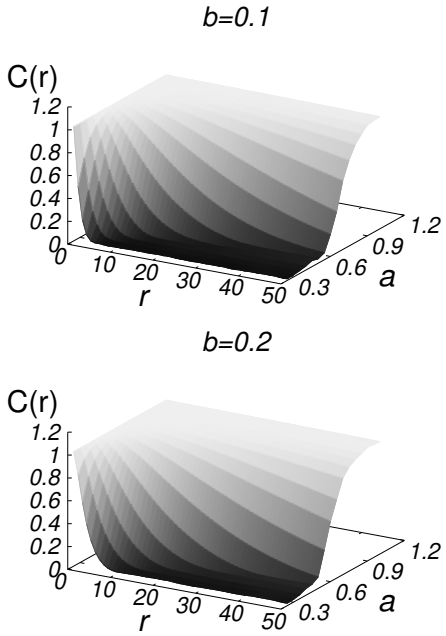

Figure 1: Autocorrelation function $C(r)$ versus r and a for $b = 0.1$ and $b = 0.2$.

P_j of each discrete eigenvalue j. Instead, we use distinct samples to calculate an average participation function $\langle P \rangle$. Specifically, for a given energy E, the average $\langle ... \rangle$ is calculated using all the data obtained within a small energy window, i.e., considering all the eigenvalues in the region $[E - \delta E/2, E + \delta E/2]$ with $\delta E \approx 0.05$.

We are able to gain further insight into the nature of the eigenstates by using the transfer matrix formalism [1, 28, 35]. This method allows us to calculate the localization length $\lambda = \{\lim_{N\to\infty}(1/N)\log[|X_N K(0)|/|K(0)|]\}^{-1}$. We stress that $K(0) = \binom{f_1}{f_0}$ represents a generic initial condition and X_N denotes the product of all transfer matrices. The behavior of λ is similar to that observed for P_j; λ is constant for localized states and proportional to N for extended modes.

The time evolution of an arbitrary one-magnon wavepacket $|\Psi(t = 0)\rangle = \sum_{n=1}^{N} y_n(t = 0)|n\rangle$ is obtained using $y_n(t) = \sum_j \{M_j f_n^j e^{-iE_j t}\}$ where $M_j = \sum_{n=1}^{N} y_n(t = 0) f_n^j$. The time-dependent magnon position is thus given by $\langle n \rangle(t) = \sum_{n=1}^{N}(n|y_n(t)|^2)$.

3. Results

We begin by examining the density of states, averaged participation number $\langle P \rangle$, and the inverse of the localization length $(1/\lambda)$ for $H = 0$, $b = 0.1$, and

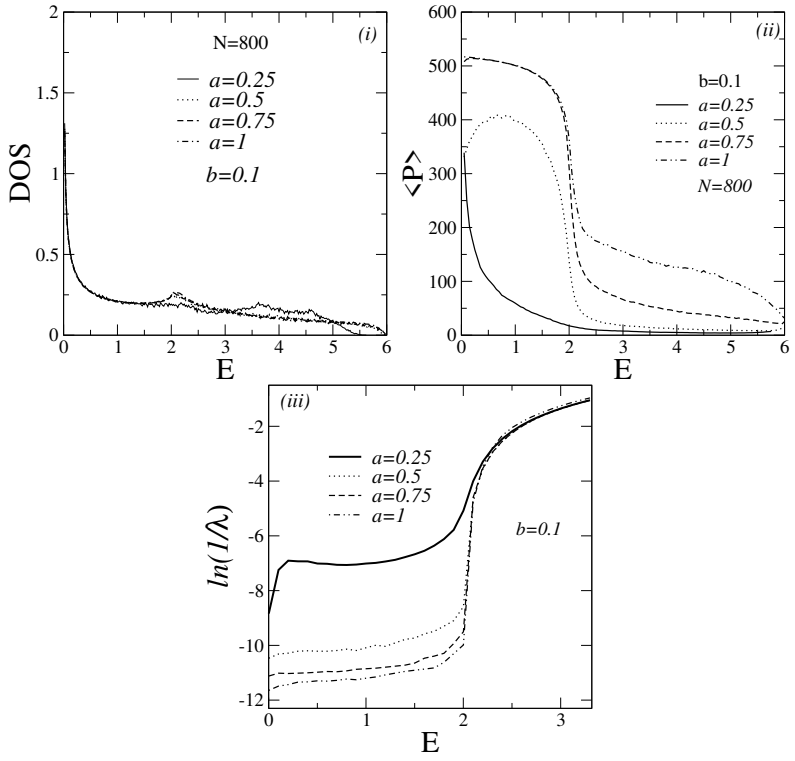

Figure 2: (i) Density of states (DOS), (ii) averaged participation number $\langle P\rangle$, and (iii) logarithm of the inverse of the localization length $1/\lambda$ for $H = 0$, $b = 0.1$, and $a = 0.25$ up to $a = 1$.

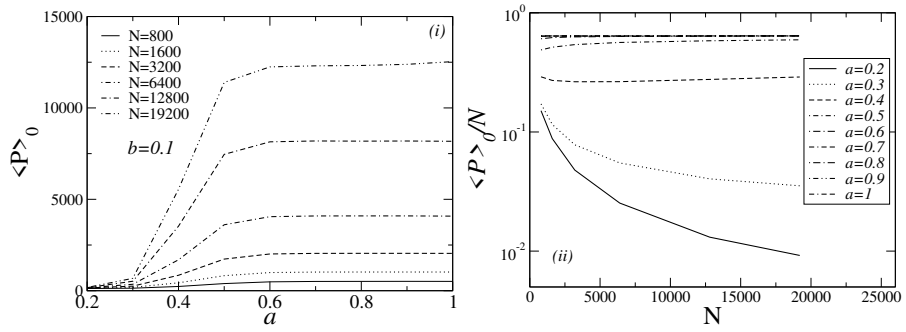

Figure 3: (i) Averaged participation number $\langle P\rangle_0$ for $E \lesssim 2$ versus a for $b = 0.1$, $H = 0$, and $N = 800$ up to 19200. (ii) Finite size scaling of $\langle P\rangle_0$ for $b = 0.1$ and several values of a. Here, the modes from $E = 0$ to $E = 0.1$ are not included because of the localization-length anomaly.

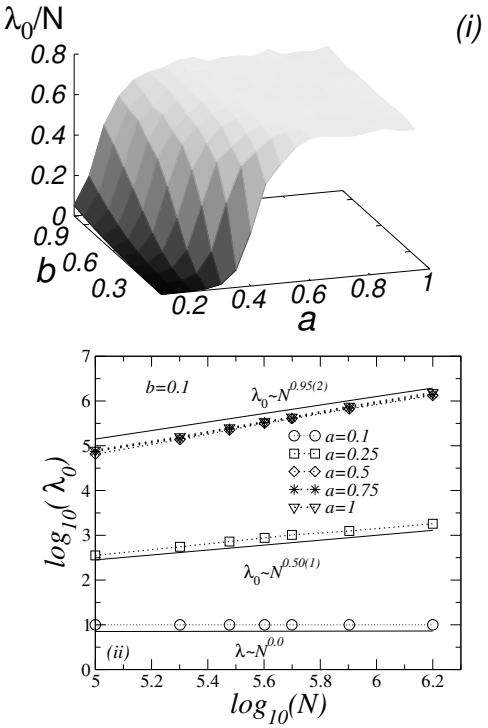

Figure 4: (i) Scaled λ_0/N versus a and b. (ii) Finite size scaling of λ_0 for $b = 0.1$ and several values of a. Calculations were done for $H = 0$.

$a = 0.25$, increasing up to $a = 1$. We used numerical diagonalization with $N = 800$ spins over 200 distinct samples, The transfer matrix procedure was in turn applied to $N = 3 \times 10^5$ spins throughout.

The main findings are summarized in Fig. 2. Our analysis indicates that the allowed energy levels are within $E \in [0, 6]$. Moreover, both the participation number and the inverse of the localization length show that for low-energy levels ($E \lesssim 2$) and strong correlations ($a \to 1$), the localization length is increased. Particularly, for small values of a the participation number is greatly enhanced at $E = 0$ [see the $a = 0.25$ curve in Fig. 2(ii)]. The Heisenberg spin model we investigate here supports an anomalous mode at that level (see e.g. Refs. [31, 32]). Thus, for energies close to $E = 0$, the typical wavelength of the spin states increases dramatically, making them less susceptible to scattering by disorder. As a result, these modes exhibit a large localization length, even in the regime of weak correlations.

With those properties in mind, we conduct a finite size scaling of $\langle P \rangle_0$ and λ_0 within this energy range (with subscript 0 denoting that). In Figure 3(i), we plot the former quantity versus a, considering $b = 0.1$, $N = 800$, up to

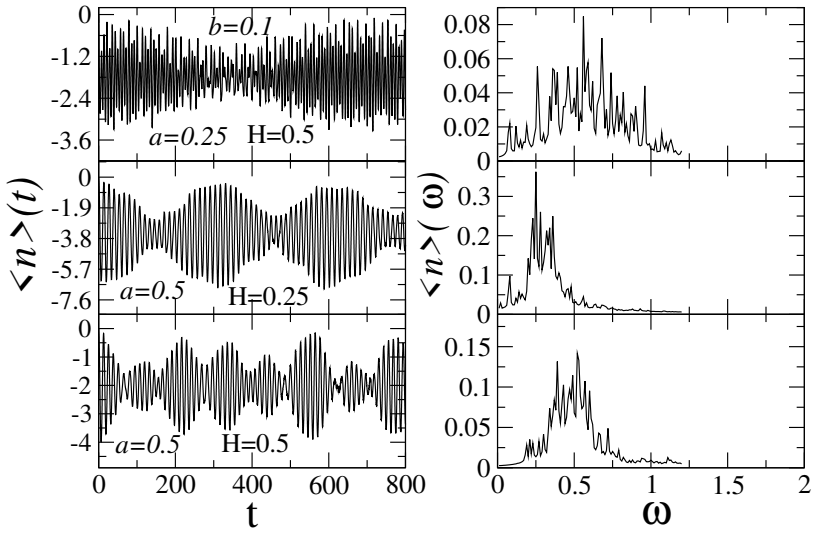

Figure 5: Left panel: The magnon position over time for $a = 0.25, 0.5$ and $H = 0.5$. Calculations were done for $b = 0.1$. Right panel: the Fourier transform of the magnon position.

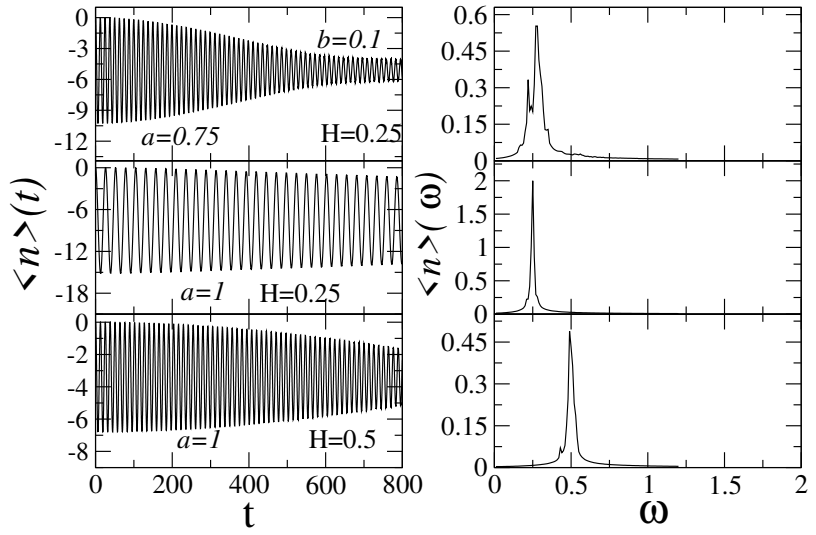

Figure 6: Left panel: The magnon position over time for $a = 0.75, 1$ and $H = 0.25, 0.5$. Calculations were done for $b = 0.1$. Right panel: the Fourier transform of the magnon position.

$N = 19200$. We clearly observe a significant growth in the participation with N for $a \geq 0.5$. In this range, the results indicate very weak localization, with the

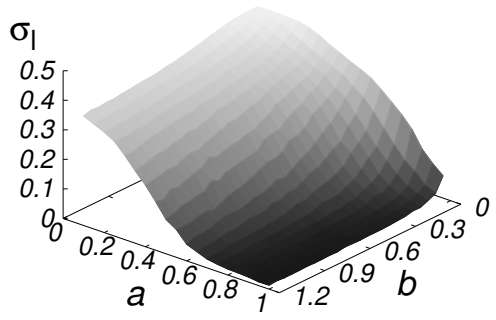

Figure 7: The local disorder versus a and b computed in a small fraction of the spin chain.

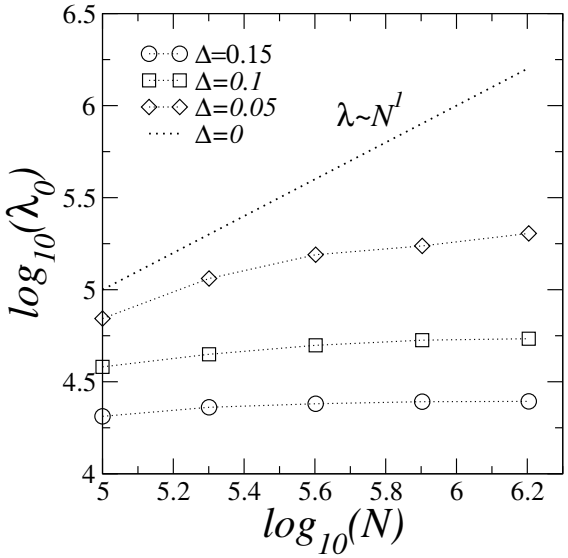

Figure 8: Localization length λ_0 versus N (in log-scale) for the uncorrelated case with weak disorder ($\Delta = 0, 0.15, 0.1, 0.05$).

average size of the eigenstates being of the order of the size of the chain. For a values below 0.5, the participation shows weak dependence on N, signalizing the presence of localized states. In Figure 3(ii), a more detailed description involving the rescaled participation $\langle P\rangle_0/N$ as a function of system size N is showed. We see that, indeed, for $a \geq 0.5$, the average participation exhibits an almost linear behavior with N. We mention that in Fig. 3 the modes around $E = 0$ (up to $E = 0.1$) are excluded due to the localization-length anomaly [31].

We emphasize that the calculations of the participation number were limited

to small or intermediate values of N as exact diagonalization was employed. However, within this context, the calculations of the localization length provide us with the opportunity to consider large systems. In Fig. 4(i), the scaled localization length λ_0/N for $E \leq 2$ versus a and b is depicted. It shows that for significant range of a and b values, the localization length is of the order of the system size. In Fig. 4(ii), we perform a finite size scaling analsis of λ_0 for $b = 0.1$ and $a = 0.1$ up to $a = 1$. For $a = 0.1$, the localization length remained roughly independent of N, indicating strong localization. As a increases, the localization length follows the trend and eventually acquires a nearly linear dependency on N, namely $\lambda_0 \propto N^{0.95}$ for $a \geq 0.5$. These results suggest the onset of localization at the thermodynamic limit, with $\lambda_0/N \to 0$ as $N \to \infty$. However, strictly speaking, we can only affirm that this limit implies an extremely weak degree of localization (an almost extended mode) within the system sizes considered in our calculations. We note that the results for $b > 0.1$ are qualitatively the same.

We now move on to explore the time dynamics of system in the presence of a magnetic field $H > 0$. For this, we prepare an initial wave packet having a Gaussian shape, $y_n(t = 0) = We^{-|n-N/2|^2/4}$, where W is a normalization constant. In Figs. 5 and 6 (left panels), we plot the expected magnon position over time for several values of a and H, with fixed $b = 0.1$. The numerical solution of the time-dependent Schrödinger equation was done using direct calculations of the evolution operator e^{-iHt}, with the norm I of the wave function remained stable, $|I - 1| < 10^{-10}$, for all simulations. In the figures, we observe a characteristic oscillatory pattern very similar to Bloch oscillations. This class phenomena is often studied in electronic models but it has also been observed in the context of magnons [30, 36].

One of the main approaches to characterize Bloch oscillations is by calculating their characteristic frequencies. The Fourier transform of the magnon position, $\langle n \rangle(\omega)$, is displayed in the right panels of Figs. 5 and 6. Note that, for $a \leq 0.5$, the oscillatory pattern contains a wide range of frequencies in the region of $\omega < 1$. For $a = 0.5$, a wide distribution is centered around the frequencies $\omega \approx H$. If a increases, the Fourier spectrum becomes narrower, as seen for $a = 1$ in Fig. 6.

Now, the question arises as to whether these oscillations with frequency $\omega \approx H$ are genuine Bloch oscillations. Based on our previous analysis, these are not. The associated modes are not truly extended; rather, they are low-energy states, in which the localization length increases with N, albeit somewhat more slowly than expected in 1D systems. The presence of these extended localization lengths, combined with the applied fields allowed us to observe oscillations over extended periods. However, over significantly longer times, the oscillatory pattern will begin to deteriorate.

Last but not least, we discuss some additional properties of the correlated disorder distribution we are using and its effect on the localization properties of the Heisenberg model in smaller scales. A convenient measure is defined as $\sigma_L = \sum_{u=1}^{l=N/L} \left(\frac{d_u}{l}\right)$, where $d_u = \langle J_n^2 \rangle_L - (\langle J_n \rangle_L)^2$. In practice, we divide the chain

into l segments, each of size L, and then we calculate the width of the disorder d_u in each of these segments. The local disorder σ_L is thereby the average of the l values of d_u. The main results can be found in Fig. 7. We observe that for the region where the correlation function becomes finite, the local disorder decreases considerably, with σ_L assuming values between 0.03 and 0.05. In the literature of correlated disorder models, this aspect is sometimes pointed out as the single ingredient promoting the increase of the localization length. In some cases, it is possible to stablish a direct relationship between the localization length and the correlation function [1]. Here, however, we can argue that an uncorrelated Heisenberg chain with weak local disorder produces a more intense degree of localization compared to the correlated scenario. Let us consider, for example, the variable $Z_n = 2\cos(2\pi n/N + \phi) + \Delta R_n$, where ϕ is a random phase chosen within the interval $[0, 2\pi]$, R_n are random numbers uniformly distributed within the interval $[0, 1]$, and Δ is a tunable parameter. Again, the spin-spin coupling is obtained following the transformation introduced earlier. In general, this results in a disordered distribution with the same boundaries, but with weak local disorder (controlled by $\Delta > 0$).

In Fig. 8, a finite size analysis for λ_0 obtained via the transfer matrix method is shown. For $\Delta = 0.05$, the localization length seems to saturate more quickly for longer chains, indicating stronger localization compared to the correlated case. We emphasize that when $\Delta = 0.1, 0.15$, the local disorder is comparable to that obtained in the correlated case with $a = 1$ and $b = 0.1, 0.2$. Therefore, our calculations clearly indicate that this type of disorder distribution, characterized by generalized exponential correlations, significantly contributes to the increase of the localization length.

4. Summary

We investigated a Heisenberg model featuring correlated disorder, an ingredient which is of significant interest in various fields [2, 3]. Here, the exchange couplings between the spins followed a disordered distribution with a exponential correlations whose the effective correlation length depended on the system size. In particular, by focusing in the one-magnon subspace, we explored the energy spectrum and the nature of the eigenstates via numerical exact diagonalization and also with the aid of the transfer matrix formalism. Our results indicated that models with correlated disorder, where the effective correlation length exhibits a slower dependence on the system size, mostly support localized eigenstates. Conversely, when the effective correlation length increases at least as the square root of the system size, the eigenmodes in the low energy region become nearly delocalized.

The dependence of the localization length on the degree of correlation is a key point in our paper. Broadly speaking, for small a (close to zero), the effective localization length is a function that increases very slowly with N. As a result, in large systems, the effective region where correlations exist becomes negligible (i.e., L_0/N quickly approaches zero). This suggests that the disorder

is essentially uncorrelated, and thus, the localization length is expected to remain constant (independent of N). As a approaches 1, the correlation length L_0 begins to show a stronger dependence on the system size, and the potential exhibits more pronounced correlations spread over a larger region (which becomes comparable to the system size in the limit $a \to 1$). Consequently, the localization length takes on a non-trivial dependence on N, eventually increasing with N and even approaching a nearly linear relationship. In other words, our model, despite having a characteristic correlation length, is able to promote a growth in the localization length to levels of the order of the system size.

We also computed the consequences of a magnetic field that varies linearly with the distance. Specifically, we showed that an initial Gaussian wave packet will undergo dynamic localization characterized by an oscillatory behavior remembering Bloch oscillations under certain correlation levels, but eventually dying off in the long time limit. This provided further insights into the interplay between correlated disorder and the magnetic field on Heisenberg models. At this point it is relevant to address a few lines about the possible consequences of a random magnetic field on our findings. In general, this would introduce a random diagonal term in the Hamiltonian, thereby weakening the effects of the correlated disorder. If the disorder strength of the random magnetic field has an intensity comparable to or above the average spin coupling, then the localization length of the eigenstates is expected to decrease significantly, also affecting the anomalous low-energy states. Furthermore, the oscillatory dynamics of the wavepacket would be suppressed much earlier in time.

As far as experimental realizations of Heisenberg models are concerned, we mention that there has been substantial progress in the field of cold atoms in optical lattices [7, 8, 37], which allows for a high degree of tuning of the parameters. In addition, spin transport mediated by exchange interactions has been observed in quantum dots [38] and bulk materials [39, 40]. Furthermore, the magnetic system studied here can be readily mapped onto a tight-binding model, making coupled waveguide arrays promising candidates for the implementation. In those systems, the separation between the waveguides can effectively assume the role of the exchange couplings. Hence, in principle any disorder profile could be envisaged within such framework [6, 41, 42].

Tailored disorder correlations can drastically influence the localization properties of magnons, suggesting potential avenues for applications in condensed-matter physics, magnonics, and quantum information processing, and more.

5. Acknowledgments

This work was supported by CNPq, CNPq-Rede Nanobioestruturas, CAPES, FINEP (Federal Brazilian Agencies), FAPEAL (Alagoas State Agency), and FACEPE (Pernambuco State Agency).

References

[1] F. Izrailev, A. Krokhin, N. Makarov, Physics Reports 512 (2012) 125.

[2] A. Simonov, A.L. Goodwin, Nat. Rev. Chem. 4 (2020) 657.

[3] D. Chaney *et al.* Phys. Rev. Mater. 5 (2021) 035004.

[4] D. Neverov, A.E. Lukyanov, A.V. Krasavin, A. Vagov, M.D. Croitoru, Commun. Phys. 5 (2022) 177.

[5] K. Vynck, R. Pierrat, R. Carminati, L. S. Froufe-Pérez, F. Scheffold, R. Sapienza, S. Vignolini, J.J. Sáenz, Rev. Mod. Phys. 95 (2023) 045003.

[6] O. Dietz, U. Kuhl, H.-J. Stöckmann, N.M. Makarov, F.M. Izrailev, Phys. Rev. B 83 (2011) 134203.

[7] J. Billy *et al.* Nature 453 (2008) 891.

[8] L. Sanchez-Palencia, M. Lewenstein, Nat. Phys. 6 (2010) 87.

[9] P. Dhawan, M. Gaudig, A. Sprafke, P. Piechulla, R. B. Wehrspohn, C. Rockstuhl, Adv. Optical Mater. 12 (2024) 2302964.

[10] A. Pando, S. Gadasi, E. Bernstein, N. Stroev, A. Friesem, N. Davidson, Phys. Rev. Lett. 133 (2024) 113803.

[11] S. Thébaud, L. Lindsay, T. Berlijn, Phys. Rev. Lett. 131 (2023) 026301.

[12] J.-H. Zheng, A. Dutta, M. Aidelsburger, and W. Hofstetter, Phys. Rev. B 109 (2024) 184201.

[13] Y.-Y. Yang, Y.-J. Chang, Y.-H. Lu, K.-D. Zhu, X.-M. Jin, ACS Photonics 11 (2024) 1024.

[14] A. Duthie, S. Roy, D.E. Logan, Phys. Rev. B 106 (2022) L020201.

[15] Y. Zhao, W. Zhang, X.-G. Yan, Physica E 117 (2020) 113781.

[16] J. Chakrian, M.L. Lyra, J.R.F. Lima, Physica E 158 (2024) 115887.

[17] Y. Zhao, S. Duan, W. Zhang, Physica E 42 (2010) 1425.

[18] N.A. Khan, P. Wang, M. Jan, G. Xianlong, Sci Rep 13 (2023) 9470.

[19] V.D. Neverov, A.E. Lukyanov, A.V. Krasavin, A. Vagov, B.G. Lvov, M.D. Croitoru, Beilstein J. Nanotechnol. 15 (2024) 199.

[20] I. Vallejo-Fabila, E.J. Torres-Herrera, Phys. Rev. B 106 (2022) L220201.

[21] S. Sun, ACS Omega 8 (2023) 40456.

[22] R.H. de Bragança, L.M.T. de Moraes, A.R.C. Romaguera, J.A. Aguiar, M.D. Croitoru, The Journal of Physical Chemistry Letters 15 (2024) 2573.

[23] V.L. Quito, J.A. Hoyos, E. Miranda, Phys. Rev. B 94 (2016) 064405.

[24] X.Lin, M. Gong, Phys. Rev. A, 109 (2024) 033310.

[25] V.D. Neverov, A.E. Lukyanov, A.V. Krasavin, A. Vagov, M.D. Croitoru, Condens. Matter 9 (2024) 6.

[26] Y. Zhao, W. Zhang, X.-G. Yan, Physica E 121 (2020) 114098.

[27] M.S.S. Junior , W.V.P. de Lima, V.A. Teixeira, D.B. da Fonseca, F. Moraes, A.L.R. Barbosa, G.M.A. Almeida, F.A.B.F. de Moura, Journal of Magnetism and Magnetic Materials 579 (2023) 170880.

[28] M.O. Sales, F.A.B.F. de Moura, Physica E 45 (2012) 97.

[29] P. Pirro, V.I. Vasyuchka, A.A. Serga, B. Hillebrands, Nature Reviews Materials 6 (2021) 1114.

[30] D.M. Nunes, A. Ranciaro Neto, F.A.B.F. de Moura, Journal of Magnetism and Magnetic Materials, 410 (2016) 165.

[31] F.A.B.F. de Moura, M.D. Coutinho-Filho, E.P. Raposo, M.L. Lyra, Phys. Rev. B 66 (2002) 014418.

[32] G.M.A. Almeida, F.A.B.F. de Moura, M. L. Lyra, Quantum Inf. Process. 18 (2010) 41.

[33] Y.A. Kosevich and V.V. Gann, J. Phys.: Condens. Matter 25 (2013) 246002.

[34] S.N. Evangelou, D.E. Katsanos, Phys. Lett. A 164 (1992) 456.

[35] Y. Kati, M.V. Fistul, A.Y. Cherny, S. Flach, Phys. Rev. A 104 (2021) 053307.

[36] U.B. Hansen, O.F. Syljuåsen, J. Jensen, T.K. Schäffer, C.R. Andersen, M. Boehm, J.A. Rodriguez-Rivera, N.B. Christensen, K. Lefmann, Nature Communications 13 (2022) 2547.

[37] N. Jepsen, J. Amato-Grill, I. Dimitrova, W.W. Ho, E. Demler, W. Ketterle, Nature (London) 588 (2020) 403.

[38] Y.P. Kandel, H. Qiao, S. Fallahi, G.C. Gardner, M.J. Manfra, J.M. Nichol, Nature 573 (2019) 553.

[39] S. Sahling, G. Remenyi, C. Paulsen, P. Monceau, V. Saligrama, C. Marin, A. Revcolevschi, L.P. Regnault, S. Raymond, J.E. Lorenzo, Nature Physics 11 (2015) 255.

[40] D.J. Choi, R. Robles, S. Yan, J.A.J. Burgess, S. Rolf-Pissarczyk, J.P. Gauyacq, N. Lorente, M. Ternes, S. Loth, Nano Letters 17 (2017) 6203.

[41] Z.S. Xu, J. Gao, G. Krishna, S. Steinhauer, V. Zwiller, A.W. Elshaari, Photon. Res. 10 (2022) 2901.

[42] J. Gao, Z.S. Xu, Z. Yang, V. Zwiller, A.W. Elshaari, npj Nanophotonics 1 (2024) 34.